hep-ph/0506120
June 2005

SANCnews: Sector $ffbb$

D. Bardin*, S. Bondarenko, L. Kalinovskaya*, G. Nanava*****, L. Rumyantsev******, and W. von Schlippe*******

* *IFJ im. Henryka Niewodniczańskiego, PAN*
ul. Radzikowskiego 152, 31-342 Kraków,
on leave from Dzhelepov Laboratory for Nuclear Problems, JINR,
ul. Joliot-Curie 6, RU-141980 Dubna, Russia;
** *Bogoliubov Laboratory of Theoretical Physics, JINR,*
ul. Joliot-Curie 6, RU-141980 Dubna, Russia;
*** *on leave from IHEP, TSU, Tbilisi, Georgia;*
**** *Dzhelepov Laboratory for Nuclear Problems, JINR,*
ul. Joliot-Curie 6, RU-141980 Dubna, Russia;
***** *Petersburg Nuclear Physics Institute,*
Gatchina, RU-188300 St. Petersburg, Russia.

Abstract

In this paper we describe the implementation of processes $f_1\bar{f}_1ZZ \to 0$ and $f_1\bar{f}_1HZ \to 0$ into the framework of SANC system [1]. The f_1 stands for a massless fermion whose mass is kept non-zero only in arguments of log functions and $\to 0$ means that all 4-momenta flow inwards. The derived scalar form factors can be used for any cross channel after an appropriate replacement of their arguments (s,t,u). As in [1], we present the covariant and helicity amplitudes for these processes: for the former only in the annihilation channel $f_1\bar{f}_1 \to ZZ$, while for the latter in annihilation $f_1\bar{f}_1 \to HZ$ and decay $H \to Zf_1\bar{f}_1$ channels. We briefly describe additional precomputation modules which were not covered in Ref. [1]. For the decay channel $H \to Zf_1\bar{f}_1$ we present and discuss exhaustive numerical results.

* Supported in part by EU grant MTKD-CT-2004-510126, in the partnership with CERN PH/TH Division.
,* Supported in part by INTAS grant N° 03-51-4007.

1 Introduction

In this paper we continue to describe the computer system `SANC` *Support of Analytic and Numerical Calculations for experiments at Colliders* intended for semi-automatic calculations of realistic and pseudo-observables for various processes of elementary particle interactions at the one-loop precision level.

Here we consider the implementation of several processes of $ffbb \to 0$ kind in the spirit of the first description of the `SANC` system (see [1] and references therein).

The present level of the system is realized in the version `v.1.10`. Compared to the version `v.1.00`, it is upgraded both physics-wise and computer-wise. As far as physics is concerned it contains an upgraded treatment of $u\bar{d} \to l^+\nu_l$ and $d\bar{u} \to l^-\bar{\nu}_l$ processes (see Ref. [2]) and a complete implementation of $F \to f + f_1 + \bar{f'}_1$ CC decays up to numbers and MC generators. (Here F and f stand for massive fermions and f_1 and $\bar{f'}_1$ for massless fermions.) Although the version `1.10` tree literally contains only $t \to b + l^+ + \nu_l$ decay, any decay of the kind $F \to f + f_1 + \bar{f'}_1$ may be treated in a similar manner and we are going to implement them into the next versions. The description of these CC decays will be given elsewhere [3].

New in version `1.10` are also several $f_1 f_1 bb$ processes, to whose implementation this paper is devoted. We describe here two of them: $f_1\bar{f}_1 ZZ \to 0$ and $f_1\bar{f}_1 HZ \to 0$, the latter one being used in two channels — annihilation and decay.

In the annihilation channel, these processes were considered in the literature extensively (see, for instance, [4] and [5]–[6]), however, we are not aware of the literature devoted to the H decay channel.

These processes are relevant for H search at LHC: the processes $f_1\bar{f}_1 \to ZZ$ are one of the backgrounds while the one-loop calculations of the decay $H \to Zf_1\bar{f}_1$ are being used for an improved treatment of the decay $H \to 4\mu$ for an intermediate Higgs mass interval 130 GeV $\leq M_H \leq$ 150 GeV, Ref. [7].

Furthermore, in the spirit of the adopted `SANC` approach, all $ffbb$ processes might be computed with off shell bosons thereby allowing their use also as building blocks for future studies of $5 \to 0$ processes.

The process $f_1\bar{f}_1 ZZ$ is very similar to the processes $ffb\gamma$ ($b = \gamma,\ Z,\ H$) whose precomputation was described in detail in Ref. [1]. Its tree level amplitude is represented by two diagrams in t and u channels, Fig. 1.

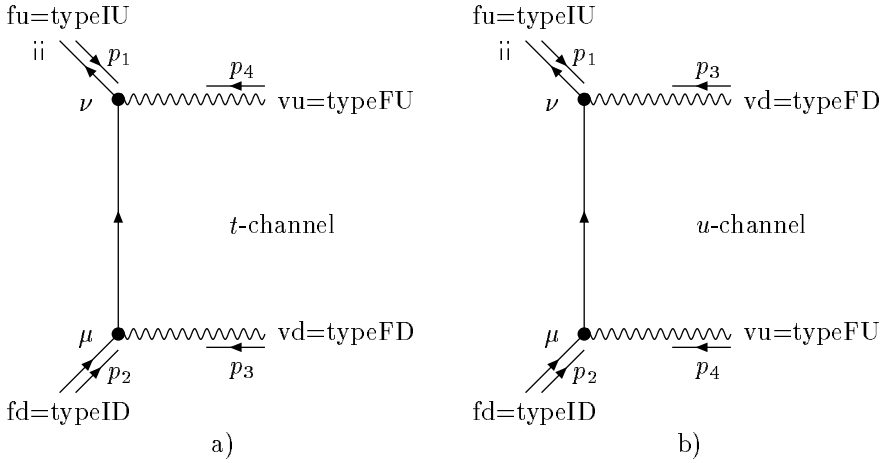

Figure 1: Born $ffHZ(ZZ)$ diagrams, t and u channels.

For the process $f_1\bar{f}_1 \to HZ$ these two diagrams do not contribute in the tree approximations since fermion f_1 is considered to be massless. However, in this case there exists an s channel amplitude, Fig. 2. All $ffbb$ processes are fully implemented at Level 1 of analytical calculations. Several new modules which

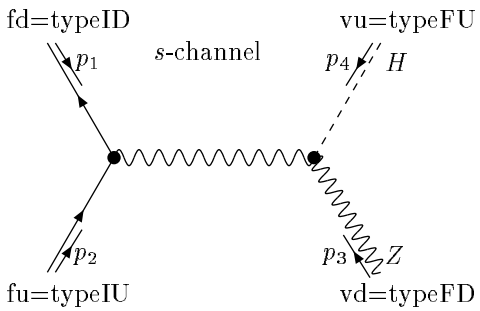

Figure 2: Born $ffHZ$ diagrams, s channel.

compute the contribution of the bbb vertices to $ffbb$ processes are added to the precomputation tree, as well as three other modules relevant for the s channel diagram.

The modified "Precomputation" tree is shown in the Fig. 5 in section 3.

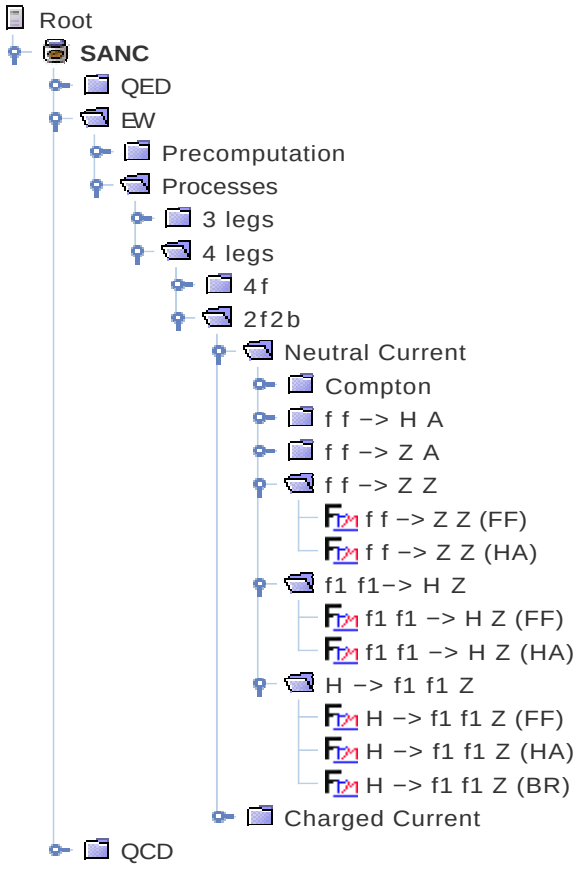

Figure 3: New processes in EW part.

The modified branch **2f2b** for the "Processes" tree is shown in Fig. 3. It contains two new sub-menus $f_1\bar{f}_1ZZ$ and $f_1\bar{f}_1HZ$ which in turn are branched into scalar Form Factors (FF) and Helicity Amplitudes (HA) (two for the process $f_1\bar{f}_1HZ$ corresponding to two annihilation and decay channels) and the accompanying Bremsstrahlung contributions (BR) for the decay channel.

The process $H \to Zf_1\bar{f}_1$ is implemented also at Level 2, where the `s2n.f` package produces the result in the "Semi Analytic" mode of the Numerical Form window (see Fig. 20 of Ref. [1]). The work on its "Monte Carlo" mode at Level 3 is in progress.

The paper is organized as follows:

In section 2 we describe the covariant (CA) and helicity amplitudes for new $ffbb$ processes available in `version 1.10`.

Section 3 contains a brief description of new precomputation modules and of several new intrinsic `SANC` procedures which are used by these precomputation modules.

In section 4 we describe in some more detail the renormalization procedure for the $f_1\bar{f}_1HZ \to 0$ process, *i.e.* calculation of FFs, and in section 5 the calculation of the accompanying Bremsstrahlung, in the semi-analytic mode.

Section 6 contains our numerical results for the decay channel $H \to Zf_1\bar{f}_1$. The numerical results and comparison for annihilation channels will be presented elsewhere.

2 Amplitude Basis, Scalar Form Factors, Helicity Amplitudes

2.1 Introduction

In this section we continue the presentation of formulae for the amplitudes of $ffbb$ processes started in section 2 of Ref. [1]. As usual, we begin with the calculation of CAs corresponding to a result of the straightforward computation of *all* diagrams contributing to a given process at the one-loop level. It is represented in a certain *basis of structures*, made of strings of Dirac matrices and external momenta, contracted with polarization vectors of vector bosons. The amplitude is parameterized by a number of FFs, which we denote by $\mathcal{F}$ with an index labeling the corresponding structure. The number of FFs is by construction equal to the number of structures, however, for the cases presented below some of the FFs might be equal, so the number of independent FFs may be less than the number of structures. For the existing tree level structures the corresponding FFs have the form

$$\mathcal{F} = 1 + \frac{\alpha}{4\pi s_W^2}\tilde{\mathcal{F}}, \tag{1}$$

where "1" is due to the Born level and $\tilde{\mathcal{F}}$ is due to the one-loop level. As usual, we use various coupling constants:

$$Q_f\,, \quad I_f^{(3)}\,, \quad \sigma_f = v_f + a_f\,, \quad \delta_f = v_f - a_f\,, \quad s_W = \frac{e}{g}\,, \quad c_W = \frac{M_W}{M_Z}\,, \quad etc. \tag{2}$$

Given a CA, `SANC` computes a set of HAs, denoted by $\mathcal{H}_{\lambda_1\lambda_2\lambda_3\ldots}$, where $\lambda_1\lambda_2\lambda_3\ldots$ denote the signs of particle spin projections onto a quantization axis.

2.2 $ff \to ZZ$ process

For definiteness, we present the CA of the process $f(p_2)\bar{f}(p_1) \to Z(p_3)Z(p_4)$ in the annihilation channel, see Fig. 1. It contains 10 left (γ_+) and 10 right (γ_-) structures:

$$\begin{aligned}
\mathcal{A}_{ffzz} \;=\; k_0 \Bigg\{ \Bigg[\bar{v}(p_1) \Big(& \not{p}_3\gamma_+(p_1)_\mu(p_1)_\nu \mathcal{F}_1^+(s,t) + \not{p}_3\gamma_+(p_1)_\mu(p_2)_\nu \mathcal{F}_2^+(s,t) \\
& + \not{p}_3\gamma_+(p_1)_\nu(p_2)_\mu \mathcal{F}_3^+(s,t) + \not{p}_3\gamma_+(p_2)_\mu(p_2)_\nu \mathcal{F}_4^+(s,t) + \not{p}_3\gamma_+\delta_{\mu\nu}\mathcal{F}_5^+(s,t) \\
& + \gamma_\mu\not{p}_3\gamma_\nu\gamma_+\mathcal{F}_6^+(s,t) + \gamma_\mu\gamma_+(p_1)_\nu\mathcal{F}_7^+(s,t) + \gamma_\mu\gamma_+(p_2)_\nu\mathcal{F}_8^+(s,t) \\
& + \gamma_\nu\gamma_+(p_1)_\mu\mathcal{F}_9^+(s,t) + \gamma_\nu\gamma_+(p_2)_\mu\mathcal{F}_{10}^+(s,t) \Big) u(p_2)\,\varepsilon_\nu^Z(p_3)\varepsilon_\mu^Z(p_4) \Bigg] \\
& + \Big[\gamma_+ \to \gamma_-\,,\; \mathcal{F}_i^+ \to \mathcal{F}_i^- \Big] \Bigg\},
\end{aligned} \tag{3}$$

where

$$k_0 = -\frac{ig^2}{8c_W^2} \qquad \text{and} \qquad \gamma_\pm = I \pm \gamma_5\,. \tag{4}$$

Furthermore,

$$Q^2 = (p_1+p_2)^2 = -s, \qquad T^2 = (p_2+p_3)^2 = -t, \qquad U^2 = (p_2+p_4)^2 = -u. \tag{5}$$

Now we give the explicit form of the CA in the tree (Born) approximation:

$$\begin{aligned}\mathcal{A}^{Born}_{ff ZZ} &= k_0 \left\{ \left[\sigma_f^2 \bar{v}\left(p_1\right) \left(\frac{T^2+U^2}{T^2U^2}\,\gamma_\mu \not{p}_3 \gamma_\nu \gamma_+ + \frac{2}{T^2}\,\gamma_\mu \gamma_+ (p_2)_\nu \; + \frac{2}{U^2} \left(\not{p}_3 \gamma_+ \delta_{\mu\nu} \right.\right.\right. \right. \\ & \left. \left. \left. -\gamma_\mu \gamma_+ (p_1)_\nu + \gamma_\nu \gamma_+ (p_1)_\mu + \gamma_\nu \gamma_+ (p_1)_\mu + \gamma_\nu \gamma_+ (p_2)_\mu \right) \right) u\left(p_2\right) \varepsilon_\nu^Z(p_3) \varepsilon_\mu^Z(p_4) \right] \\ & + \left[\sigma_f^2 \to \delta_f^2,\ \gamma_+ \to \gamma_- \right] \Bigg\}. \end{aligned} \tag{6}$$

Note that this is decomposed into 16 structures of 20 and is highly asymmetric in T^2 and U^2. This is due to our choice of the 4-momentum p_3 and of the ordering of Lorentz indices μ and ν.

Among the 20 FFs there are four identities:

$$\mathcal{F}_4^{\pm}(s,t) = \mathcal{F}_1^{\pm}(s,t), \quad \mathcal{F}_{10}^{\pm}(s,t) = -\mathcal{F}_7^{\pm}(s,t). \tag{7}$$

Therefore, there are 16 independent FFs but 18 independent non-zero HAs for $f_1\bar{f}_1 \to ZZ$ process:

$$\begin{aligned}
\mathcal{H}_{+-+-} &= \frac{k_0^s}{2} \sin\vartheta_z c_+ \left\{ +\frac{s}{4} c_- \beta \left[2\mathcal{F}_1^+(s,t) - \mathcal{F}_2^+(s,t) - \mathcal{F}_3^+(s,t) \right] - 2\mathcal{F}_7^+(s,t) + \mathcal{F}_8^+(s,t) - \mathcal{F}_9^+(s,t) \right\}, \\
\mathcal{H}_{+--+} &= \frac{k_0^s}{2} \sin\vartheta_z c_- \left\{ +\frac{s}{4} c_+ \beta \left[2\mathcal{F}_1^+(s,t) - \mathcal{F}_2^+(s,t) - \mathcal{F}_3^+(s,t) \right] + 2\mathcal{F}_7^+(s,t) - \mathcal{F}_8^+(s,t) + \mathcal{F}_9^+(s,t) \right\}, \\
\mathcal{H}_{-++-} &= \frac{k_0^s}{2} \sin\vartheta_z c_- \left\{ -\frac{s}{4} c_+ \beta \left[2\mathcal{F}_1^-(s,t) - \mathcal{F}_2^-(s,t) - \mathcal{F}_3^-(s,t) \right] - 2\mathcal{F}_7^-(s,t) + \mathcal{F}_8^-(s,t) - \mathcal{F}_9^-(s,t) \right\}, \\
\mathcal{H}_{-+-+} &= \frac{k_0^s}{2} \sin\vartheta_z c_+ \left\{ -\frac{s}{4} c_- \beta \left[2\mathcal{F}_1^-(s,t) - \mathcal{F}_2^-(s,t) - \mathcal{F}_3^-(s,t) \right] + 2\mathcal{F}_7^-(s,t) - \mathcal{F}_8^-(s,t) + \mathcal{F}_9^-(s,t) \right\}, \\
\mathcal{H}_{+-++} &= k_0^s \sin\vartheta_z \left\{ -\frac{s}{8} \sin^2\vartheta_z \beta \left[2\mathcal{F}_1^+(s,t) - \mathcal{F}_2^+(s,t) - \mathcal{F}_3^+(s,t) \right] \right. \\
&\quad \left. -\beta \mathcal{F}_5^+(s,t) + \beta_- \mathcal{F}_6^+(s,t) + \cos\vartheta_z \mathcal{F}_7^+(s,t) + \frac{1}{2} c_- \mathcal{F}_8^+(s,t) + \frac{1}{2} c_+ \mathcal{F}_9^+(s,t) \right\}, \\
\mathcal{H}_{+---} &= k_0^s \sin\vartheta_z \left\{ -\frac{s}{8} \sin^2\vartheta_z \beta \left[2\mathcal{F}_1^+(s,t) - \mathcal{F}_2^+(s,t) - \mathcal{F}_3^+(s,t) \right] \right. \\
&\quad \left. -\beta \mathcal{F}_5^+(s,t) + \beta_+ \mathcal{F}_6^+(s,t) + \cos\vartheta_z \mathcal{F}_7^+(s,t) - \frac{1}{2} c_+ \mathcal{F}_8^+(s,t) - \frac{1}{2} c_- \mathcal{F}_9^+(s,t) \right\}, \\
\mathcal{H}_{-+--} &= k_0^s \sin\vartheta_z \left\{ +\frac{s}{8} \sin^2\vartheta_z \beta \left[2\mathcal{F}_1^-(s,t) - \mathcal{F}_2^-(s,t) - \mathcal{F}_3^-(s,t) \right] \right. \\
&\quad \left. +\beta \mathcal{F}_5^-(s,t) - \beta_- \mathcal{F}_6^-(s,t) - \cos\vartheta_z \mathcal{F}_7^-(s,t) - \frac{1}{2} c_- \mathcal{F}_8^-(s,t) - \frac{1}{2} c_+ \mathcal{F}_9^-(s,t) \right\}, \\
\mathcal{H}_{-+++} &= k_0^s \sin\vartheta_z \left\{ +\frac{s}{8} \sin^2\vartheta_z \beta \left[2\mathcal{F}_1^-(s,t) - \mathcal{F}_2^-(s,t) - \mathcal{F}_3^-(s,t) \right] \right. \\
&\quad \left. +\beta \mathcal{F}_5^-(s,t) - \beta_+ \mathcal{F}_6^-(s,t) - \cos\vartheta_z \mathcal{F}_7^-(s,t) + \frac{1}{2} c_+ \mathcal{F}_8^-(s,t) + \frac{1}{2} c_- \mathcal{F}_9^-(s,t) \right\}, \\
\mathcal{H}_{+-+0} &= \frac{1}{2} k_0^s k_1^+ \left\{ -\frac{s}{4} c_- \beta \left[-2\cos\vartheta_z \mathcal{F}_1^+(s,t) - \beta_-^c \mathcal{F}_2^+(s,t) + \beta_+^c \mathcal{F}_3^+(s,t) \right] \right.
\end{aligned}$$

$$
\begin{aligned}
& +\beta_-^2\,\mathcal{F}_6^+(s,t)-\left(\beta_+^c-c_-\right)\mathcal{F}_7^+(s,t)-c_-\mathcal{F}_8^+(s,t)+\beta_-^c\,\mathcal{F}_9^+(s,t)\Big\},\\
\mathcal{H}_{+-0+} &= \frac{1}{2}k_0^s k_1^-\Big\{-\frac{s}{4}c_+\beta\left[2\cos\vartheta_z\mathcal{F}_1^+(s,t)+\beta_-^c\,\mathcal{F}_2^+(s,t)-\beta_+^c\mathcal{F}_3^+(s,t)\right]\\
& +4\frac{M_Z^2}{s}\mathcal{F}_6^+(s,t)-\left(\beta_+^c+c_+\right)\mathcal{F}_7^+(s,t)-\beta_-^c\mathcal{F}_8^+(s,t)-c_+\mathcal{F}_9^+(s,t)\Big\},\\
\mathcal{H}_{+-00} &= k_0^s\frac{s}{M_Z^2}\sin\vartheta\Big\{-\frac{1}{16}s\beta\left[2\beta_+^c\beta_-^c\,\mathcal{F}_1^+(s,t)+(\beta_-^c)^2\mathcal{F}_2^+(s,t)+(\beta_+^c)^2\mathcal{F}_3^+(s,t)\right]\\
& -\beta\left[\frac{M_Z^2-\frac{s}{2}}{s}\mathcal{F}_5^+(s,t)-\frac{M_Z^2}{s}\mathcal{F}_6^+(s,t)\right]+\frac{1}{4}\big(2\beta_+^c\mathcal{F}_7^+(s,t)+\beta_-^c\left[\mathcal{F}_8^+(s,t)-\mathcal{F}_9^+(s,t)\right]\big)\Big\},\\
\mathcal{H}_{+--0} &= k_0^s k_1^+\Big\{-\frac{s}{8}c_-\beta\left[-2\cos\vartheta_z\mathcal{F}_1^+(s,t)-\beta_-^c\,\mathcal{F}_2^+(s,t)+\beta_+^c\mathcal{F}_3^+(s,t)\right]\\
& -2\frac{M_Z}{s}\mathcal{F}_6^+(s,t)-\frac{1}{2}\left(\beta_+^c-c_-\right)\mathcal{F}_7^+(s,t)-\frac{1}{2}\beta_-^c\,\mathcal{F}_8^+(s,t)+\frac{1}{2}c_-\mathcal{F}_9^+(s,t)\Big\},\\
\mathcal{H}_{+--0} &= \frac{1}{2}k_0^s k_1^-\Big\{-\frac{s}{4}c_+\beta\left[2\cos\vartheta_z\mathcal{F}_1^+(s,t)+\beta_-^c\,\mathcal{F}_2^+(s,t)-\beta_+^c\mathcal{F}_3^+(s,t)\right]\\
& +2\left(2\frac{M_Z}{s}-\beta_+\right)\mathcal{F}_6^+(s,t)-\left(\beta_+^c+c_+\right)\mathcal{F}_7^+(s,t)+c_+\mathcal{F}_8^+(s,t)+\beta_-^c\,\mathcal{F}_9^+(s,t)\Big\},\\
\mathcal{H}_{-++0} &= \frac{1}{2}k_0^s k_1^-\Big\{+\frac{s}{4}c_+\beta\left[-2\cos\vartheta_z\mathcal{F}_1^-(s,t)-\beta_-^c\,\mathcal{F}_2^-(s,t)+\beta_+^c\mathcal{F}_3^-(s,t)\right]\\
& -\beta_+^2\mathcal{F}_6^-(s,t)-\left(\beta_+^c+c_+\right)\mathcal{F}_7^-(s,t)+c_+\mathcal{F}_8^-(s,t)+\beta_-^c\,\mathcal{F}_9^-(s,t)\Big\},\\
\mathcal{H}_{-+0+} &= \frac{1}{2}k_0^s k_1^+\Big\{+\frac{s}{4}c_-\beta\Big(2\cos\vartheta_z\mathcal{F}_1^-(s,t)+\beta_-^c\,\mathcal{F}_2^-(s,t)-\beta_+^c\mathcal{F}_3^-(s,t)\Big)\\
& -4\frac{M_Z^2}{s}\mathcal{F}_6^-(s,t)-\left(\beta_+^c-c_-\right)\mathcal{F}_7^-(s,t)-\beta_-^c\mathcal{F}_8^-(s,t)+c_-\mathcal{F}_9^-(s,t)\Big\},\\
\mathcal{H}_{-+00} &= \frac{1}{4}k_0^s\frac{s}{M_Z^2}\sin\vartheta_z\Big\{+\frac{s}{4}\beta\Big(+\beta_+^c\beta_-^c\,\mathcal{F}_1^-(s,t)+(\beta_-^c)^2\mathcal{F}_2^-(s,t)+(\beta_+^c)^2\mathcal{F}_3^-(s,t)\\
& -\frac{8}{s}\left[\left(1-2\frac{M_Z}{s}\right)\mathcal{F}_5^-(s,t)+2\frac{M_Z}{s}\mathcal{F}_6^-(s,t)\right]\Big)-2\beta_+^c\mathcal{F}_7^-(s,t)-\beta_-^c\left[\mathcal{F}_8^-(s,t)-\mathcal{F}_9^-(s,t)\right]\Big\},\\
\mathcal{H}_{-+0-} &= k_0^s k_1^-\Big\{-\frac{s}{8}c_+\beta\Big(2\cos\vartheta_z\mathcal{F}_1^-(s,t)+\beta_-^c\,\mathcal{F}_2^-(s,t)-\beta_+^c\mathcal{F}_3^-(s,t)\Big)\\
& +2\frac{M_Z}{s}\mathcal{F}_6^-(s,t)-\frac{1}{2}\left(\beta_+^c+c_+\right)\mathcal{F}_7^-(s,t)-\frac{1}{2}\beta_-^c\mathcal{F}_8^-(s,t)-\frac{1}{2}c_+\mathcal{F}_9^-(s,t)\Big\},\\
\mathcal{H}_{-+-0} &= k_0^s k_1^+\Big\{+\frac{s}{8}c_-\beta\Big(2\cos\vartheta_z\mathcal{F}_1^-(s,t)+\beta_-^c\,\mathcal{F}_2^-(s,t)-\beta_+^c\mathcal{F}_3^-(s,t)\Big)\\
& -\left(2\frac{M_Z}{s}+\beta_-\right)\mathcal{F}_6^-(s,t)-\frac{1}{2}\left(\beta_+^c-c_-\right)\mathcal{F}_7^-(s,t)-\frac{1}{2}c_-\mathcal{F}_8^-(s,t)+\frac{1}{2}\beta_-^c\,\mathcal{F}_9^-(s,t)\Big\},\\
\mathcal{H}_{++++} &= \mathcal{H}_{+++0}=\mathcal{H}_{+++-}=\mathcal{H}_{++0+}=\mathcal{H}_{++00}=\mathcal{H}_{++0-}=\mathcal{H}_{++-+}=\mathcal{H}_{++-0}=0,\\
\mathcal{H}_{++--} &= \mathcal{H}_{--++}=\mathcal{H}_{--+0}=\mathcal{H}_{--+-}=\mathcal{H}_{--0+}=\mathcal{H}_{--00}=\mathcal{H}_{--0-}=\mathcal{H}_{---+}=0,\\
\mathcal{H}_{---0} &= \mathcal{H}_{----}=0. \qquad (8)
\end{aligned}
$$

Here we use the following shorthand notation:

$$k_0^s = k_0 s, \qquad k_1^{\pm} = \frac{\sqrt{s}}{\sqrt{2}M_Z} c_{\pm}, \qquad c_{\pm} = 1 \pm \cos\vartheta_Z,$$

$$\beta_{\pm} = \beta \pm 1, \qquad \beta_{\pm}^c = \beta \pm \cos\vartheta_Z, \qquad \beta = \frac{\sqrt{\lambda(s, M_Z^2, M_Z^2)}}{s}. \tag{9}$$

The number 18 is the product of 2 initial massless helicity states and 3×3 states for both final Z bosons.

2.3 $f_1\bar{f}_1 \to HZ$ process

There are six structures for the $f_1\bar{f}_1 \to HZ$ process if the fermion mass is neglected

$$\mathcal{A}_{f f HZ} = k\left\{\left[\bar{v}(p_1)\left(\gamma_\nu\gamma_+\sigma_f\mathcal{F}_0^+(s,t) + \not{p}_3\gamma_+(p_1)_\nu\mathcal{F}_1^+(s,t) + \not{p}_3\gamma_+(p_2)_\nu\mathcal{F}_2^+(s,t)\right)u(p_2)\,\varepsilon_\nu^Z(p_3)\right]\right.$$
$$\left. + \left[\sigma_f \to \delta_f,\ \gamma_+ \to \gamma_-,\ \mathcal{F}_i^+(s,t) \to \mathcal{F}_i^-(s,t)\right]\right\}, \tag{10}$$

where
$$k = -\frac{ig^2}{4c_W^2}\frac{M_Z}{M_Z^2 - s}\,. \tag{11}$$

The structures for the decay $H \to Zf_1\bar{f}_1$ may be obtained by simple replacement of 4-momenta $p_1 \to -p_3$, $p_2 \to -p_4$, $p_4 \to -p_1$ ($p_3 \to p_2$) of the structures 10.

As far as HAs is concerned, we present them in both channels: annihilation and decay.

2.3.1 HAs in annihilation channel $f_1\bar{f}_1 \to HZ$

There are 6 HAs in this case:

$$\begin{aligned}
\mathcal{H}_{+-+} &= k_0^s c_+\left\{k_1^-\left[\mathcal{F}_2^+(s,t) - \mathcal{F}_1^+(s,t)\right] - 4\sigma_e\mathcal{F}_0^+(s,t)\right\},\\
\mathcal{H}_{-++} &= -k_0^s c_-\left\{k_1^+\left[\mathcal{F}_1^-(s,t) - \mathcal{F}_2^-(s,t)\right] + 4\delta_e\mathcal{F}_0^-(s,t)\right\},\\
\mathcal{H}_{+--} &= -k_0^s c_-\left\{k_1^+\left[\mathcal{F}_1^+(s,t) - \mathcal{F}_2^+(s,t)\right] + 4\sigma_e\mathcal{F}_0^+(s,t)\right\},\\
\mathcal{H}_{-+-} &= k_0^s c_+\left\{k_1^-\left[\mathcal{F}_2^-(s,t) - \mathcal{F}_1^-(s,t)\right] - 4\delta_e\mathcal{F}_0^-(s,t)\right\},\\
\mathcal{H}_{+-0} &= k_0^s k_2\left\{\sqrt{\lambda(s,M_Z^2,M_H^2)}\left[\beta_+^c\mathcal{F}_1^+(s,t) + \beta_-^c\mathcal{F}_2^+(s,t)\right] + 4\sigma_e\mathcal{F}_0^+(s,t)\right\},\\
\mathcal{H}_{-+0} &= -k_0^s k_2\left\{\sqrt{\lambda(s,M_Z^2,M_H^2)}\left[\beta_+^c\mathcal{F}_1^-(s,t) + \beta_-^c\mathcal{F}_2^-(s,t)\right] + 4\delta_e\mathcal{F}_0^-(s,t)\right\},\\
\mathcal{H}_{+++} &= \mathcal{H}_{++0} = \mathcal{H}_{++-} = \mathcal{H}_{--+} = \mathcal{H}_{--0} = \mathcal{H}_{---} = 0,
\end{aligned} \tag{12}$$

where

$$k_0^s = k_0\frac{1}{\sqrt{2}}\frac{\sqrt{s}M_Z}{s - M_Z^2}, \qquad k_1^{\pm} = \sqrt{\lambda(s,M_Z^2,M_H^2)}c_{\pm}, \qquad k_2 = \frac{s + M_Z^2 - M_H^2}{\sqrt{2}\sqrt{s}M_Z}\sin\vartheta_Z,$$

$$c_{\pm} = 1 \pm \cos\vartheta_Z, \qquad \beta_{\pm}^c = \beta \pm \cos\vartheta_Z, \qquad \beta = \frac{\sqrt{\lambda(s,M_Z^2,M_H^2)}}{s + M_Z^2 - M_H^2}\,. \tag{13}$$

2.3.2 HAs in the decay channel $H \to Z f_1 \bar{f}_1$

The six HAs in this case are somewhat different from the previous case:

$$\begin{aligned}
\mathcal{H}_{++-} &= k_0^s\Big\{k_1\left[\mathcal{F}_1^-(s,t)-\mathcal{F}_2^-(s,t)\right]-4\delta_f c_-\mathcal{F}_0^-(s,t)\Big\},\\
\mathcal{H}_{+-+} &= k_0^s\Big\{k_1\left[\mathcal{F}_2^+(s,t)-\mathcal{F}_1^+(s,t)\right]-4\sigma_f c_+\mathcal{F}_0^+(s,t)\Big\},\\
\mathcal{H}_{-+-} &= k_0^s\Big\{k_1\left[\mathcal{F}_1^-(s,t)-\mathcal{F}_2^-(s,t)\right]+4\delta_f c_+\mathcal{F}_0^-(s,t)\Big\},\\
\mathcal{H}_{--+} &= k_0^s\Big\{k_1\left[\mathcal{F}_2^+(s,t)-\mathcal{F}_1^+(s,t)\right]+4\sigma_f c_-\mathcal{F}_0^+(s,t)\Big\},\\
\mathcal{H}_{0+-} &= k_0^s k_2\Big\{\ \sqrt{\lambda(M_H^2,M_Z^2,s)}\left[\beta_+^c\mathcal{F}_1^-(s,t)+\beta_-^c\mathcal{F}_2^-(s,t)\right]-4\delta_e\mathcal{F}_0^-(s,t)\Big\},\\
\mathcal{H}_{0-+} &= k_0^s k_2\Big\{-\sqrt{\lambda(M_H^2,M_Z^2,s)}\left[\beta_+^c\mathcal{F}_1^+(s,t)+\beta_-^c\mathcal{F}_2^+(s,t)\right]+4\sigma_e\mathcal{F}_0^+(s,t)\Big\},\\
\mathcal{H}_{+++} &= \mathcal{H}_{+--}=\mathcal{H}_{0++}=\mathcal{H}_{0--}=\mathcal{H}_{-++}=\mathcal{H}_{---}=0.
\end{aligned} \tag{14}$$

Here,

$$\begin{aligned}
k_0^s &= k_0\frac{1}{\sqrt{2}}\frac{\sqrt{s}M_Z}{M_Z^2-s}, \qquad k_1=\sqrt{\lambda(M_H^2,M_Z^2,s)}\sin^2\vartheta_l, \qquad k_2=\frac{\left(M_H^2-M_Z^2-s\right)}{\sqrt{2}\sqrt{s}M_Z}\sin\vartheta_l,\\
c_\pm &= 1\pm\cos\vartheta_l, \qquad \beta_\pm^c=\beta\pm\cos\vartheta_l, \qquad \beta=\frac{\sqrt{\lambda(M_H^2,M_Z^2,s)}}{M_H^2-M_Z^2-s}\,.
\end{aligned} \tag{15}$$

The number 6 is the product of 2 initial massless helicity states and 3 states of the final Z boson.

Furthermore,

$$s = M^2_{f_1\bar{f}_1}\ , \tag{16}$$

is the invariant mass of the two fermions f_1, varying in the limits $4m^2_{f_1} \le s \le (M_H - M_Z)^2$; and t is another independent kinematical variable, depending on s and an angle ϑ_l, varying in the limits $0 \le \vartheta_l \le \pi$

$$t = M_Z^2 + \frac{1}{2}\left[M_H^2 - M_Z^2 - s - \sqrt{\lambda(M_H^2,M_Z^2,s)}\cos\vartheta_l\right]. \tag{17}$$

The kinematical diagram of the process is shown in Fig. 4.

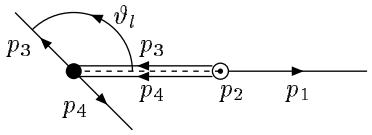

Figure 4: $H \to Z f_1 \bar{f}_1$ decay kinematics.

The Higgs boson with momentum p_2 at rest, decays back-to-back into a Z boson with momentum p_1 and a fermionic compound with 4-momentum $p_3 + p_4$ and invariant mass s. This compound decays in its own rest frame into two back-to-back fermions with ϑ_l being the angle between p_3 in the compound rest frame and the direction of flight of the Z boson.

3 Precomputation news

The modified part of the "Precomputation" tree of `version 1.10` is shown in Fig. 5 with all sub-menus, which were not changed, closed. In this section we briefly discuss what every new module does.

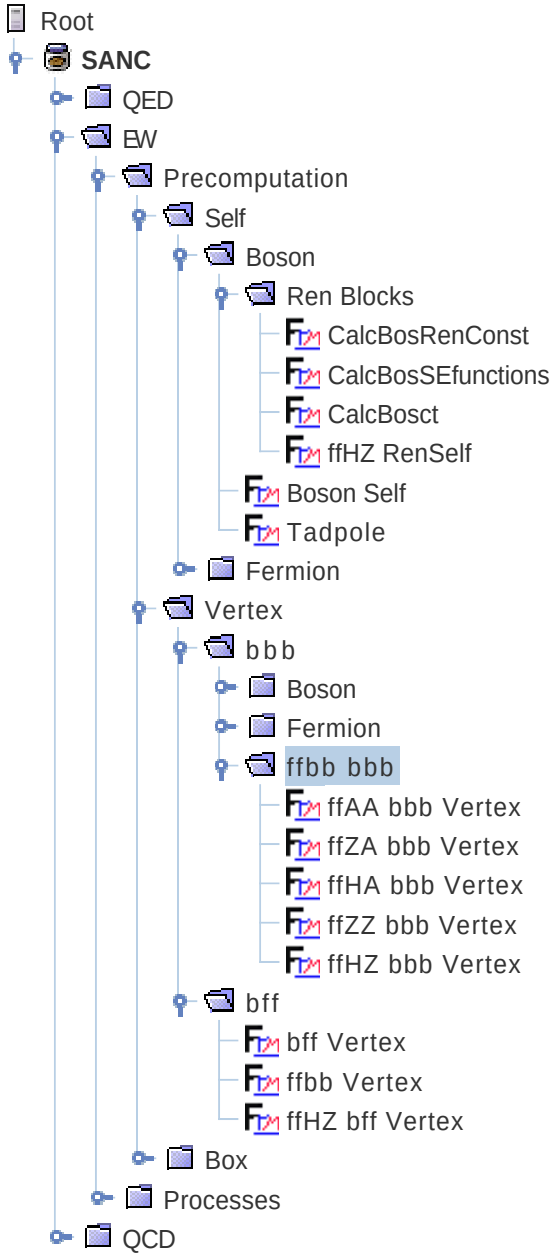

Figure 5: New EW precomputation modules.

First, we added a new folder accessible via menu sequence **EW** $\rightarrow$ **Precomputation** $\rightarrow$ **Vertex** $\rightarrow$ **bbb** $\rightarrow$ **ffbb bbb** with five modules **ffXX bbb Vertex, XX=AA,ZA,HA,ZZ,HZ** which compute three boson vertices of four topologies (see Fig. 11 of Ref. [1]) to the corresponding $ffbb$ processes, Fig. 6. The results of their calculations are saved to ffXX*.sav files to be loaded by corresponding modules computing FFs via chains **EW** $\rightarrow$ **Processes** $\rightarrow$ **4-legs** $\rightarrow$ **2f2b** $\rightarrow$ **Neutral Current** for the $ffXX \rightarrow 0$ processes.

These three boson diagrams contain both *bosonic* and *fermionic* components. The latter are precomputed by the modules **bbb Vertex** in **Boson** and **Fermion** folders of the same level on the tree. Five modules of **ffbb bbb** folder load them and then apply tedious calculations involving in some cases the Schouten identity. There are many peculiarities in these calculations, forcing us to have an individual module for each $ffbb$ process. Note also that if the corresponding process has a Born-level s channel exchange as in Fig. 2, then the contribution of one-loop vertices is supplemented by the relevant counterterm cross.

In the modules under discussion a summation over the exchanged boson B is performed. In general, four neutral bosons $B = \gamma, Z, \phi^0$ and H could contribute if the fermion mass is not neglected, otherwise, only γ and Z contribute.

For the processes $ffAA \rightarrow 0$, $ffZA \rightarrow 0$ and $ffHA \rightarrow 0$ the "left" bff vertex diagram, shown in Fig. 7 does not contribute, since in these cases the "right" vertex does not exist at the tree level. In general, and this is indeed the case for the processes $ffZZ \rightarrow 0$ and $ffHZ \rightarrow 0$, the "right" vertex exists at the tree level for $B = Z, \phi^0$, therefore, the dressed "left" vertex has to be added to the precomputation tree. Note that it does not contribute for massless fermion if $B = \phi^0$. For $ffHZ \rightarrow 0$ this vertex is accessible via menu sequence **EW** $\rightarrow$ **Precomputation** $\rightarrow$ **Vertex** $\rightarrow$ **bff** $\rightarrow$ **ffHZ bff Vertex**. For the $ffZZ \rightarrow 0$ process, only $B = H$ contributes, but then, for the massless f_1, the dressed "left" vertex vanishes, this is why we do not add the corresponding module in the latter case.

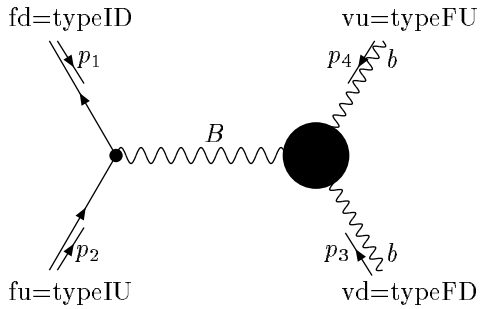

Figure 6: "Right" bbb vertex in $ffbb$ processes.

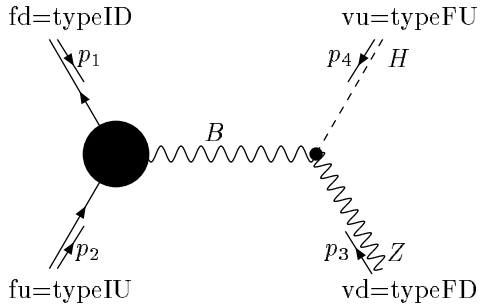

Figure 7: "Left" bff vertex in $ffbb$ processes.

The presence of an s channel tree level diagram in the process $f_1\bar{f}_1 HZ \to 0$ (Fig. 2) forces us to take into account two more self energy diagrams, Fig. 8.

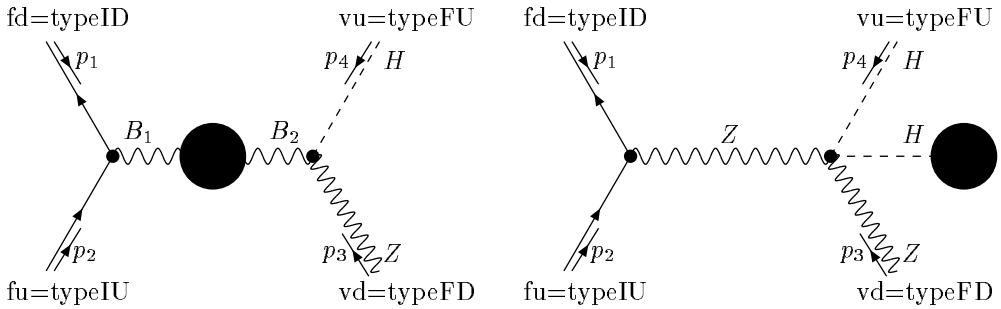

Figure 8: Self energy $ffHZ$ diagrams.

The first one is accessible via menu chain: **Self** $\to$ **Boson** $\to$ **Ren Blocks** $\to$ **ffHZ Ren Self**. Here $B_1 = \gamma, Z, \phi^0$ and $B_2 = Z, \phi^0$; again ϕ^0's do not contribute for massless fermions. As will be explained in the next section, the second diagram is better to be combined with the "right" vertex, Fig. 6.

Note that nothing is changed, compared to $ffXA$ processes, as far as boxes are concerned. So, the **Box** sub-menu is as `in version 1.00`.

The new modules contain calls to several new *intrinsic* procedures which are not described in this news letter. We postpone its description until the next version release.

4 Renormalizaton for $ffHZ \to 0$ process

In this section we describe how to use the FORM module which computes FFs for the process $f_1 f_f HZ \to 0$. This description is supposed to help a user to understand the other modules computing FFs for any $ffbb \to 0$ process.

First of all, to use our basic declaration and notation we begin the file with

```
#include Declar.h
#call Globals()
```

and define types of external particles, see Figs. 1 and 2.

```
#ifdef 'typeIU';  *  'fu'
#ifdef 'typeID';  *  'fd'
#ifdef 'typeFU';  *  'vu'
#ifdef 'typeFD';  *  'vd'
#define typeIDp "{2*('typeID'%2)-1+'typeID'}";  * 'fdp'
```

Secondly, we fix four main steering flags to define the calculational scheme:

1. define xi: xi = 0 to test gauge invariance in R_ξ, or xi = 1 to work in $\xi = 1$ gauge;
2. define on: on = 0 external photons are off mass-shell, or on = 1 photons are on mass-shell;
3. define mf: mf = 0 ignore fermion mass (*i.e.* pm('fd')=0), or mf = 1 it is not ignored;
4. define mp: mp = 0 partner fermion mass, pm('fdp')=0, or mp = 1 it is not ignored.

Actually, for the considered process, $f_1 \bar{f}_1 HZ \to 0$ only ξ and mp definitions are meaningful since there are no external photons and we ignore the mass of external fermions throughout the calculations, but the partner fermion mass may be kept non zero.

The ideology of building blocks (BB) is the key element for SANC development. The information about the main precomputed BB is stored in basic ***.sav** files (BSF). Note that for 4-particle $ffbb$ processes all the BBs are 4-legs by construction. This trick will greatly simplify the procedure of projection of the covariant amplitude onto an independent basis of structures.

Moreover, for the future development it is necessary to upgrade the database of the collected information area SANC: fields of program modules, fields of procedures and the bank of BSF.

Any module computing FFs starts from loading of the calculated BB from the bank of BSF. These BSF contain the precomputed objects: self energies, vertices and boxes typically with off-shell bosons.

They are precomputed not only to accelerate the calculations. Although all BSF may be, in principle, precomputed online, we remind that in some cases the CPU time for calculating of off-shell boxes in R_ξ gauge takes many hours, see section 3.4 of Ref. [1]. In such cases precomputation is strictly prohibited.

We recall also that our precomputation procedure has indeed several levels; in the modules computing FFs we tend to use the results of the last level which contains already renormalized BBs: propagators and vertices, *i.e.* taking into account relevant *counterterms* and *special vertices*, [8]. However, they are full of residual UV poles and ξ dependent terms, which cancel in the sum for an one-loop covariant amplitude of a physical process. This is why we still use to word "renormalization" in connection with a module computing FFs.

Typically, the loading of BSFs is organized in the several steps. Let us consider the example of **H → f1 f1 Z** module, see the tree in Fig. 5.

- step self

  Here we manipulate with objects from the BSF ffHZSelfschxi'xi''fu''fd''vu''vd'.sav

  We extract from its volume the BB of bosonic self energy in the s-channel, BSEsch'fu''fd''vu''vd' see left diagram in Fig. 8.

- step vertex

  Moving further over the renormalization procedure at this step we load three BSFs:
  ffHZVertbffxi'xi''fu''fd''vu''vd'.sav;
  ffHZVertbbbxi'xi''fu''fd''vu''vd'.sav;
  ffbbVertxi'xi'on'on'mf'mf'mp'mp''fu''fd''vu''vd'.sav.

  From these BSFs we extract various types of vertices:
  — VertBff'i''fu''fd''vu''vd' with i=1,2,3,4 standing for ξ_A, ξ_Z, ξ_W, and no ξ *vertex clusters* originating from the diagram of Fig. 7;
  — Vertbbbbos'fu''fd''vu''vd' and Vertbbbfer'fu''fd''vu''vd' — the *bosonic* and *fermionic* components of three-boson vertices shown in the diagram Fig. 6, where the former contains counterterms, special vertex as well as the right diagram in Fig. 8; the latter tadpoles cancel the ξ_Z dependence of the three-boson vertices, giving an opportunity to assign this contribution to i=3; finally, the fermionic component should be naturally assigned to i=4;
  — abelian Vert'I''i' and non-abelian vert'I''i' vertex clusters in t and u channels I=t,u with cluster index i=1,2,3,4 and k=22,33,24,42,44, see section 3.4.2 of Ref. [1] for a description of the latter.

- step boxes

  Here the most complex building blocks — off-shell boxes are loaded from four BSFs:
  ffbb3T1xi'xi'on'on'mf'mf'mp'mp''fu''fd''vd''vu'.sav;
  ffbb3T3xi'xi'on'on'mf'mf'mp'mp''fu''fd''vu''vd'.sav;
  ffbb22T5xi'xi'on'on'mf'mf'mp'mp''vd''fd''vu''fu'.sav;
  ffbb33T5xi'xi'on'on'mf'mf'mp'mp''vd''fd''vu''fu'.sav.

  They contain precomputed boxes of the topology T1 from the expression S3T1'xi''on''mf''mp''fu''fd''vd''vu', the boxes of the topology T3 from the expression S3T3'xi''on''mf''mp''fu''fd''vu''vd', and of the topology T5 with cluster index $k1 = 2, 3$, *i.e.* with virtual Z and W bosons from the expression S'k1''k1'T5'xi''on''mf''mp''vd''fd''vu''fu'.

  Only those box topologies and clusters are loaded which give a non-zero contribution for $m_{f_1} = 0$.

- step Sum

  To finish the preparation for renormalization procedure we sum all contributions. Four expressions, Sum'i', corresponding to cluster index i=1,2,3,4 are being constructed here. The first three of them may carry only one gauge parameter each, the latter carries none.

After construction of four Sum'i', the module continues with various kinds of transformations (in particular, involving an algebra of Gram determinants) which are supposed to demonstrate the cancellation of gauge parameter dependences in first three Sum1,2,3 and the cancellation of the residual UV poles between FFs with cluster indices i=3 and i=4.

At a point commented `Preparing Structures for obtaining FFs:` the six basis elements of the CA Eq(10) are created and the 6×4 FFs are projected out of this CA.

The final step is formatting of the BSF FFf1f1HZ.sav with six FFs summed back over cluster indices — FFgpi and FFgmi ($i = 0, 1, 2$) — for subsequent processing by s2n.f software.

5 Bremsstrahlung in $H \to Z f_1 \bar{f}_1$ decay

In this section we present the list of short final results for the contribution of accompanying Bremsstrahlung to the decay channel $H \to Z f_1 \bar{f}_1$ under consideration.

We begin with the tree level diagram, Fig. 9:

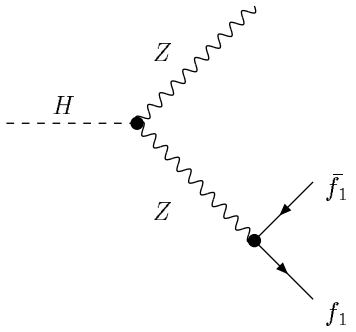

Figure 9: The $H \to Z f_1 \bar{f}_1$ decay, tree level diagram.

The corresponding tree level double differential width, depending on two kinematical variables s, ϑ_l discussed in section 2.3.2 and kinematics shown in Fig. 4, reads

$$\frac{d^2\Gamma^{\rm Born}}{ds\, d\cos\vartheta_l} = k_B \left\{ \left[\left(1 - \frac{s}{M_H^2}\right)^2 - 2s\frac{M_Z^2}{M_H^4} - 1 + \left(1 - \frac{M_Z^2}{M_H^2}\right)^2 \right] \sin^2\theta_l + 8s\frac{M_Z^2}{M_H^4} \right\}, \tag{18}$$

where

$$k_B = \frac{1}{128}\frac{G_F^2}{\pi^3}\left(v_f^2 + a_f^2\right)\frac{\sqrt{\lambda\left(M_H^2, M_Z^2, s\right)}\, M_Z^4 M_H}{\left|M_Z^2 - iM_Z\Gamma_Z - s\right|^2}. \tag{19}$$

There are only two final state Bremsstrahlung diagrams, Fig. 10:

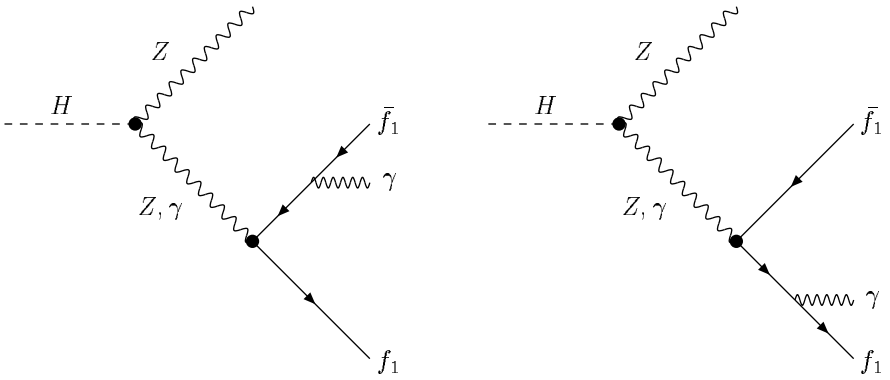

Figure 10: The $H \to Z f_1 \bar{f}_1$ decay, Bremsstrahlung.

The fully differential phase space is characterized by five kinematical variables which we choose as follows:

$$d\Phi^{(3)} = \frac{ds}{2\pi}\frac{d\tau}{2\pi}\, d\Phi_1^{(2)}\, d\Phi_2^{(2)}\, d\Phi_3^{(2)}. \tag{20}$$

The 3-step kinematical cascade develops as a sequence of three 2-body decays shown in Fig. 11,

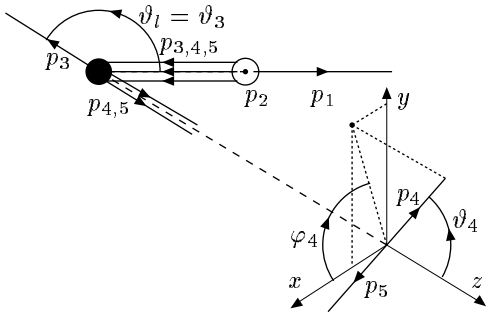

Figure 11: Bremsstrahlung kinematics.

with corresponding two body phase spaces:

$$\begin{aligned} d\Phi_1^{(2)} &= \frac{1}{8\pi}\frac{\sqrt{\lambda(M_H^2, M_Z^2, M_H^2)}}{M_H^2}\,, \\ d\Phi_2^{(2)} &= \frac{1}{8\pi}\frac{\sqrt{\lambda(s, \tau, m_{f_1}^2)}}{s}\,\frac{1}{2}\,d\cos\vartheta_3\,, \\ d\Phi_3^{(2)} &= \frac{1}{8\pi}\frac{\sqrt{\lambda(\tau, m_{f_1}^2, 0)}}{\tau}\,\frac{1}{2}\,d\cos\vartheta_4\,\frac{1}{2\pi}d\varphi_4\,. \end{aligned} \tag{21}$$

The gauge invariant QED part of the complete one-loop EW correction is subdivided into *virtual, soft* and *hard* photon contributions. The virtual one comes from the two Born-like FFs with cluster index i=1. It is proportional to the Born width and contains infrared divergence parameterized by the photon mass λ:

$$\frac{d^2\Gamma^{\rm Virt}}{ds\,d\cos\vartheta_l} = \frac{d^2\Gamma^{\rm Born}}{ds\,d\cos\vartheta_l}\frac{\alpha}{\pi}Q_f^2\left\{-\ln\left(\frac{m_e^2}{\lambda^2}\right)\left[\ln\left(\frac{s}{m_e^2}\right)-1\right]+\frac{1}{2}\ln\left(\frac{s}{m_e^2}\right)\left[3-\ln\left(\frac{s}{m_e^2}\right)\right]+4{\rm Li}_2(1)-2\right\}. \tag{22}$$

The soft photon contribution is also proportional to the Born one; its infrared divergence cancels against virtual contribution. It contains also a log with *soft-hard separator* $\bar{\omega}$:

$$\frac{d^2\Gamma^{\rm Soft}}{ds\,d\cos\vartheta_l} = \frac{d^2\Gamma^{\rm Born}}{ds\,d\cos\vartheta_l}\frac{\alpha}{\pi}Q_f^2\left\{\left[\ln\left(\frac{m_e^2}{\lambda^2}\right)+2\ln\left(\frac{2\bar{\omega}}{m_e}\right)-\ln\left(\frac{s}{m_e^2}\right)\right]\left[\ln\left(\frac{s}{m_e^2}\right)-1\right]-{\rm Li}_2\,(1)+1\right\}. \tag{23}$$

The hard photon contribution after integration over three kinematical variables $d\varphi_4$, $d\cos\vartheta_4$ and $d\tau$ (the first two vary together in full angular 4π limits and $m_{f_1}^2 \le \tau \le (\sqrt{s}-m_{f_1})^2$) is

$$\begin{aligned} \frac{d^2\Gamma^{\rm Hard}}{ds\,d\cos\vartheta_l} = \frac{d^2\Gamma^{\rm Born}}{ds\,d\cos\vartheta_l}\frac{\alpha}{\pi}Q_f^2\Bigg\{&-2\ln\left(\frac{2\bar{\omega}}{m_e}\right)\left[\ln\left(\frac{s}{m_e^2}\right)-1\right]-\frac{1}{2}\ln\left(\frac{s}{m_e^2}\right)\left[5-3\ln\left(\frac{s}{m_e^2}\right)\right]-3{\rm Li}_2(1)+\frac{1}{4}\Bigg\} \\ &+k_B\frac{\alpha}{\pi}Q_f^2\left[\left(1-\frac{s}{M_H^2}\right)^2+10s\frac{M_Z^2}{M_H^4}-1+\left(1-\frac{M_Z^2}{M_H^2}\right)^2\right]. \end{aligned} \tag{24}$$

The total QED correction, sum of above three contributions, is free not only of infrared divergence and of soft-hard separator, but also free of final fermion mass singularity in accordance with the KLN theorem [9]–[10].

$$\frac{d^2\Gamma^{\rm Total}}{ds\, d\cos\vartheta_l} = \frac{d^2\Gamma^{\rm Born}}{ds\, d\cos\vartheta_l}\frac{\alpha}{\pi}Q_f^2 + k_{_B}\frac{\alpha}{\pi}Q_f^2\left[\left(1-\frac{s}{M_H^2}\right)^2 + 10s\frac{M_Z^2}{M_H^4} - 1 + \left(1-\frac{M_Z^2}{M_H^2}\right)^2\right]. \qquad (25)$$

Finally, if one integrates over $d\cos\vartheta_l$, the well known Z decay correction factor restores:

$$\frac{d\Gamma^{\rm Total}}{ds} = \frac{d\Gamma^{\rm Born}}{ds}\left[1+\frac{3}{4}\frac{\alpha}{\pi}Q_f^2\right]. \qquad (26)$$

Therefore, the QED part of the correction is small, $\sim 0.2\%$.

6 Numerical results and comparison

Let us turn to the complete one-loop EW correction. The upper part of Table 1 shows the double differential decay width for the decay $H \to Z\mu^+\mu^-$ for $M_{_H}$ =130 GeV and for a set of s and $\cos\vartheta_l$. The lower part of the Table 1 shows the single differential decay width after an integration over $\cos\vartheta_l$.

$2m_\mu \le \sqrt{s} \le (M_{_H} - M_Z)$, α scheme					
$d^2\Gamma/ds\, d\cos\vartheta_l \cdot 10^8$, GeV^{-1}					
		$\sqrt{s}$, GeV			
	$\cos\vartheta_l$	1	3	10	38
Born		0.0438391	0.0460521	0.0619837	0.0903068
Born+1-loop	± 0.9	0.5074381	0.1002282	0.0699933	0.0981556
δ		10.5645619	1.1662886	0.1216893	0.0851191
Born		0.1724379	0.1761864	0.1829820	0.0918593
Born+1-loop	± 0.5	0.5024053	0.2236158	0.1985445	0.0998374
δ		1.9121884	0.2678408	0.0836500	0.0851174
Born		0.2298480	0.2342821	0.2369991	0.0925524
Born+1-loop	0.0	0.5004122	0.2789556	0.2561597	0.1005884
δ		1.1765618	0.1900923	0.0801635	0.0851184
$d\Gamma/ds \cdot 10^9$, GeV^{-1}					
1)		3.0660233	3.1364235	3.2995218	1.8325481
2)		10.064194	4.1063021	3.5893752	1.9917237
$\delta\%$		228	30.9	8.78	8.89

Table 1: The double differential width is multiplied by a factor of 10^8; δ is the ratio One-loop/Born; the single differential width is multiplied by a factor of 10^9 and the ratio δ is given in %.

From Table 1 it is seen that at the edges of $\cos\vartheta_l$ and near the fermionic threshold the double differential width shows a $1/s$ behaviour, typical for Coulomb interaction.

The origin of the Coulomb peak at the one-loop level may be easily understood. First we note that $H \to Z\gamma$ width does not vanish for an on-shell photon with $Q^2_\gamma = 0$, Fig. 12:

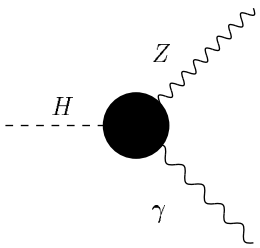

Figure 12: $H \to Z\gamma$ decay.

Therefore, the one-loop amplitude for $H \to Z f_1 \bar{f}_1$ with virtual photon exchange

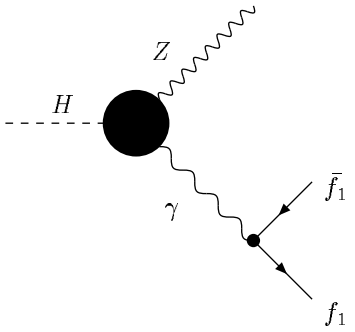

Figure 13: Compton singularity.

will show a $\sim 1/s$ behaviour (with $s = -Q^2_\gamma$). This, in turn, will lead to the $\sim 1/s$ behaviour of both the double and single differential widths. This conclusion is fully confirmed by the numbers in the Table 1.

Recalling now the limits for s : $4m^2_{f_1} \leq s \leq (M_H - M_Z)^2$, one might expect the appearance after integration over s of the big log $\ln((M_H - M_Z)^2/m^2_{f_1})$, with a final state fermion mass singularity. However, the $1/s$ region is very narrow and it is largely washed out not only by a soft cut on the variable s but even by the the plain integration over s.

Finally let us discuss the total width. In Born approximation it is $\Gamma^{\rm Born} = 5.255 \cdot 10^{-6}$ GeV, while with the complete EW corrections it is $\Gamma^{\rm Born+1-loop} = 5.733 \cdot 10^{-6}$ GeV. The correction amounts to 9.1%, which is a rather large value nonetheless.

Acknowledgements

The authors are grateful to P. Christova for a valuable discussion of Bremsstrahlung issues, to A. Arbuzov for discussion of the stability of numerical calculations and physical results and also to W. Hollik for providing us with useful references. Three of us (D.B., L.K. and G.N.) are indebted to the directorate of IFJ, Krakow, for hospitality which was extended to them in April–May 2005, when the major part of this study was done.

References

[1] A. Andonov, A. Arbuzov, D. Bardin, S. Bondarenko, P. Christova, L. Kalinovskaya, G. Nanava, and W. von Schlippe, *SANCscope — v.1.00*, to be published in Computer Physics Communications, `hep-ph/0411186`.

[2] A. Arbuzov, D. Bardin, S. Bondarenko, P. Christova, L. Kalinovskaya, G. Nanava, and R. Sadykov, *One-loop corrections to the Drell–Yan processes in SANC (I). The charged current case.* `hep-ph/0506110`.

[3] A. Arbuzov, et al. *SANCnews: Sector 4f, Charged Current*, in preparation.

[4] A. Denner and T. Sack. *Nucl. Phys.* **B306** (1988) p.221.

[5] M.L. Ciccolini, S. Dittmaier and M. Krämer, `hep-ph/0306234`.

[6] O. Brein, M. Ciccolini, S. Dittmaier, A. Djouadi, R. Harlander and M. Krämer, `hep-ph/0402003`.

[7] D. Bardin, et al. *About $H \to 4\mu$ decay in SANC*, in preparation.

[8] D. Bardin and G. Passarino, *The standard model in the making: Precision study of the electroweak interactions.* Clarendon, 1999. Oxford, UK.

[9] T. Kinoshita, J. Math. Phys. **3** (1962) 650.

[10] T. D. Lee and M. Nauenberg, Phys. Rev. **133** (1964) B1549.